INJURY BIOMECHANICS RESEARCH
Proceedings of the Thirty-Seventh International Workshop

Storage and loss modulus of brain tissue determined with the atomic force microscope

Barclay Morrison III, Benjamin S. Elkin

This paper has not been screened for accuracy nor refereed by any body of scientific peers and should not be referenced in the open literature.

ABSTRACT

Material properties are one critical requirement for accurate computational modeling of injury events. Modeling brain injuries is complicated by the brain's heterogeneous structure and measuring material properties is further complicated by the sizes of those structures. We have previously used the atomic force microscope (AFM) to measure pseudo-static mechanical properties of rat brain tissue at a spatial resolution capable of discerning between anatomical structures. We are extending these earlier studies with the AFM to measure frequency dependent properties in response to sinusoidal indentations up to 800 Hz, in some cases. Preliminary analysis indicates significant regional differences in stiffness. Brain tissue stiffness was strongly dependent on both oscillation frequency and indentation depth, reinforcing the need for nonlinear viscoelastic constitutive models to adequately describe the mechanical behavior of brain tissue. The AFM methodology, data analysis, and limitations will be discussed.

INTRODUCTION

Finite element (FE) models provide the critical link between macroscopic loading parameters and the resultant mechanical reaction at the tissue level. The input mechanical stimulus is ultimately responsible for the biological outcome. Through computational models, laboratory experiments at the tissue level can be translated to predict tissue-level responses to real-world injury scenarios. FE models are becoming increasingly important in automotive and safety system design and perhaps in the legislative domain in the future (Takhounts et al., 2003; Takhounts et al., 2008).

For computational models to accurately predict biological outcomes, they first must accurately predict the mechanical response at the tissue level, which requires appropriate material properties. Measuring material properties of the brain poses particular challenges. Brain is one of the softest tissues in the body and to measure reaction forces during testing requires either very sensitive transducers or large samples (Prange and Margulies, 2002; Gefen et al., 2003; Nicolle et al., 2004; Coats and Margulies, 2005; Hrapko et al., 2006). Brain is structurally heterogeneous with gray and white matter at the grossest level of distinction with many finer features apparent upon histological examination. The use of large samples precludes measuring the properties of these finer structures.

One motivation to measure material properties of the brain's substructures or components is that others have shown that inclusion of heterogeneous material properties in computational models provides more accurate predictions of induced tissue damage (Zhou et al., 1995). Only by inclusion of particular anatomical structures within a model can the predicted injury pattern be compared and validated against histological sections of the true injury pattern. For example, the CA3 pyramidal layer of the hippocampus is particularly vulnerable to fluid percussion injury (FPI) models of TBI (Hicks et al., 1996; Smith et al., 1997; Morales et al., 2005). Predicting this preferential cell loss in CA3 with a computational model would be a substantial step toward its validation. But, only by inclusion of a hippocampus with a CA3 subfield will that be possible.

We were further motivated to measure the mechanical properties of subregions of the brain by findings in our tissue culture injury model that CA1 and CA3 were equally vulnerable to strain-induced cell death (Morrison III et al., 2003; Cater et al., 2006). Our data were in contrast to experimental findings that CA3 was preferentially vulnerable to FPI *in vivo* (Hicks et al., 1996; Smith et al., 1997). One explanation was that our injury model induced deformation by the controlled stretch of the substrate to which the brain tissue cultures were adhered. The substrate is several orders of magnitude stiffer than the brain tissue, so its deformation is not appreciably affected by the cultured slice. In contrast, in the experimental animal models, a pressure pulse is applied to the surface of the brain, whereby the induced, local tissue strain depends on the regional mechanical properties of the brain. This heterogeneity may be as complex as the heterogeneous structure evident in histological sections. Therefore, we hypothesized that the CA3 region is more compliant than other hippocampal regions giving rise to larger local deformations and hence greater cell death in CA3 *in vivo*.

To test our hypothesis, we are in the process of using the atomic force microscope (AFM) to measure mechanical properties within specific anatomical structures of the brain.

METHODS

All animal procedures were approved by the Columbia University Institutional Animal Care and Use Committee (IACUC). Rats were anesthetized with isoflurane before the brain was immediately removed and sectioned into slices. For AFM studies, 400um sections were cut in the coronal plane with a vibrating blade microtome (Vibratome, St. Louis, MO) and plated on non-porous silicone membranes coated with laminin and poly-L-lysine, bathed in Neurobasal medium (Invitrogen), and allowed to adhere. All slices were maintained in a tissue culture incubator at 37°C, 5% CO_2, and 100% relative humidity until tested. Mechanical testing was completed within 2h of death unless otherwise noted.

All mechanical testing was performed on a heated stage to maintain the tissue at 37ºC and in CO_2 independent culture medium. An atomic force microscope (AFM; Bioscope, Veeco, Santa Barbara, CA) mounted on an inverted light microscope (IX-81; Olympus, Melville, NY) was used to measure material properties within local regions of the brain. Cantilever probes were modified with 12.5µm radius sphere and calibrated by the manufacturer (NovaScan, spring constant = 0.13-0.16 N/m). The cantilever probe was mounted on a fluid cell with a modified moisture trap cuff to ensure that media did not evaporate during the procedure. Indentations were performed with a ramp indentation at 0.01 Hz to acquire data at different indentation depths (up to 3µm). Superimposed on top of the slow ramp was a sinusoidal oscillation of the probe tip to measure frequency dependant mechanical properties as described below. Oscillatory frequencies tested were 5, 10, 50, 100, 200, 400, and in some cases 800 Hz providing approximately equally spaced frequencies in log space.

Contact point was identified from raw deflection versus displacement data (force curves) for each indentation according to our previously described methods (Elkin et al., 2007). In addition, the phase lag of the sinusoidal oscillation also provides a sensitive indicator for contact. When the tip made contact with the tissue, the phase angle between the force and displacement changed drastically as the tip transitioned from a purely viscous deflection to a material deflection. We used both methods to improve the reliability of contact point identification, but are still optimizing specifics of the algorithm.

For determination of the non-linear strain response, depth-dependent pointwise apparent elastic modulus ($\hat{E}$) was calculated using the following equation (Costa and Yin, 1999; Costa, 2003) applied to the slow, large indentations:

$$\hat{E} = \frac{3(1-\nu^2)\bullet f}{4\sqrt{R\delta_o{}^3}} \quad (1)$$

where f is the cantilever force, *R* is the spherical radius of the probe tip, δ_o is the indentation depth, and *v* is the Poisson's ratio of brain assumed to be 0.5 (Darvish and Crandall, 2001; Lippert et al., 2004).

The static equation was extended to the dynamic regime for a small oscillatory displacement superimposed on the static displacement $\delta = \delta_o + \tilde{\delta}^*$ by taking the Taylor expansion of the static solution according to published methods (Mahaffy et al., 2000; Alcaraz et al., 2003; Mahaffy et al., 2004) and retaining the oscillatory component only to give Eq. 2.

$$f^*_{osc} = 2\sqrt{R\delta_o}\,\frac{E_1^*}{(1-\nu^2)}\cdot\tilde{\delta}^* \quad (2)$$

A lock-in amplifier (SR830, Stanford Research Systems) was used to measure the phase difference between the small amplitude driving displacement of the scanner and the cantilever deflection as well as the magnitude of cantilever deflection.

To correct for cantilever dynamic drag force due to the medium, drag force was calculated from cantilever deflection, in free medium given by Eq. 3.

$$f^*_{drag} = i\varpi\cdot\gamma\cdot\tilde{\delta}^* \quad (3)$$

The depth and frequency dependent storage (*E'*) and loss (*E"*) moduli were then given by (4) where φ is the phase difference between the scanner displacement with magnitude a_d and cantilever displacement with magnitude a_r at a given indentation depth, δ_0.

$$E_1' = \frac{(1-\nu^2)}{2\sqrt{R\delta_o}}\cdot\frac{a_d k a_r\cos\varphi - k a_r^2}{a_d^2 - 2a_d a_r\cos\varphi + a_r^2}$$
$$E_1'' = \frac{(1-\nu^2)}{2\sqrt{R\delta_o}}\cdot\left[\frac{a_d k a_r\sin\varphi}{a_d^2 - 2a_d a_r\cos\varphi + a_r^2} - \varpi\cdot\gamma\right] \quad (4)$$

RESULTS

Representative storage and loss modulus is presented for one region, the middle cortex for the adult rat brain. Both E' and E" increase as the indentation frequency increases. This has been noted by others when testing larger samples of brain tissue (Arbogast and Margulies, 1997; Brands et al., 2000; Nicolle et al., 2005). In addition, dynamic modulus increases with indentation depth. We have not yet analyzed the data in terms of strain, but the dependence on indentation depth indicates that the trend will hold with respect to strain in accordance with our previously reported data from slow AFM indentations. Lastly, the data indicates that E" is larger than E' for high frequencies.

One difficulty with the dynamic AFM indentation technique is identification of contact point – the point at which the probe engages the tissue. Below are presented three cases in which the static deflection of the cantilever as it indents the tissue is compared to the in-phase (real) and out-of-phase (imaginary) components of the deflection. Raw data is presented for 400, 100, and 10Hz indentations to present the variety of challenges associated with this methodology.

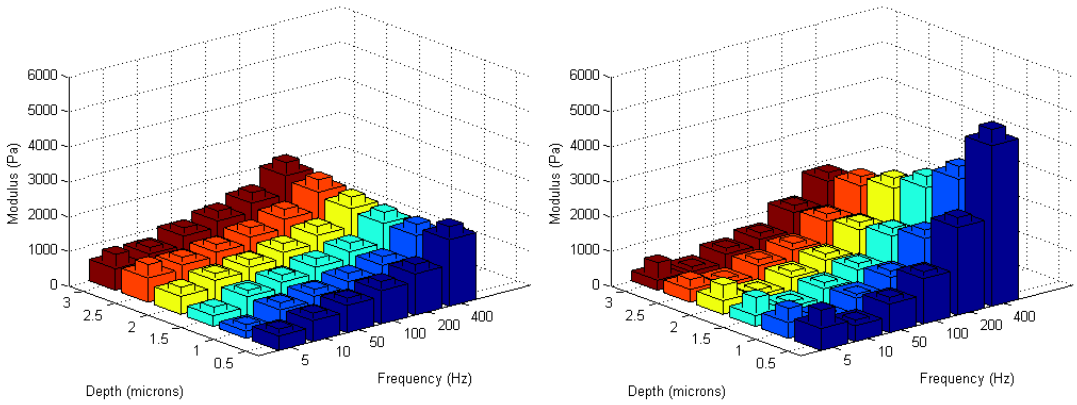

Fig. 1 Middle Cortex storage, E' (L) and loss, E" (R) modulus plotted by frequency and indentation depth. Bars are mean + SD.

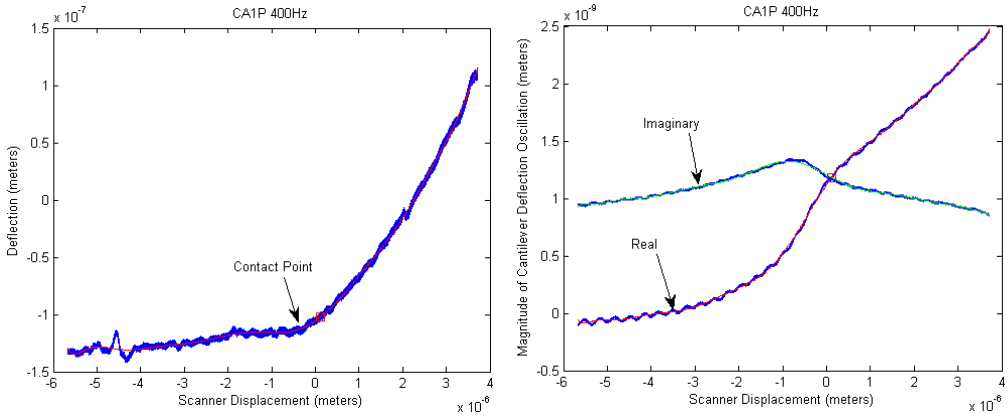

Fig. 2 Static indentation deflection plot (L) and dynamic real and imaginary deflection for the CA1 pyramidal cell layer for a 400Hz oscillation. Identification of a consistent contact point for both sets of data is challenging.

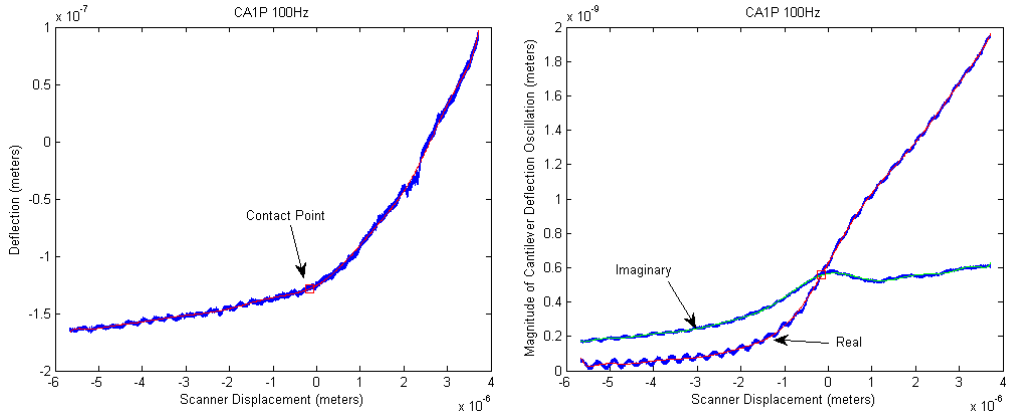

Fig. 3 Static indentation deflection plot (L) and dynamic real and imaginary deflection for the CA1 pyramidal cell layer for a 100Hz oscillation.

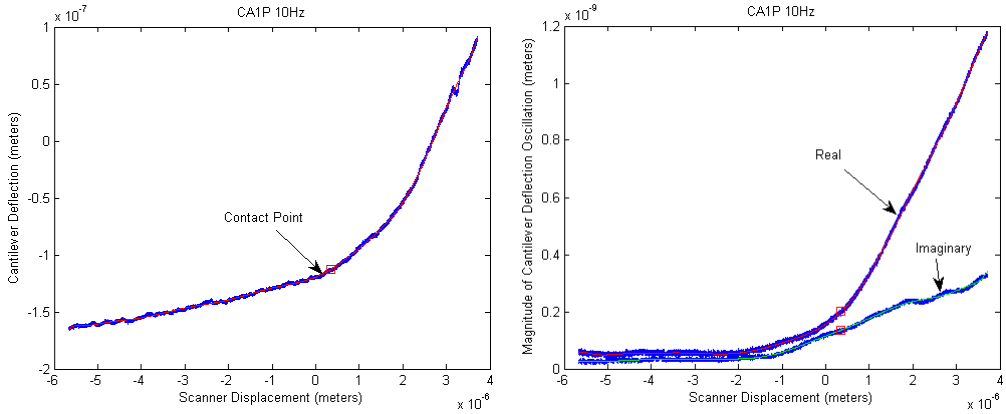

Fig. 4 Static indentation deflection plot (L) and dynamic real and imaginary deflection for the CA1 pyramidal cell layer for a 10Hz oscillation.

DISCUSSION

Finite element modeling of TBI requires certain enabling data. These include mechanical properties which are critical for predicting accurate brain deformation in response to macroscopic, whole-body loads. We have previously reported mechanical properties of the 8 day old rat hippocampus measured with the AFM (Elkin et al., 2007), as well as a follow-up study in the P10, P17, and adult rat brain (Elkin et al., 2010). The AFM is an attractive tool for measuring brain mechanical properties for several reasons including spatial and force resolution and the ability to conduct measurements in physiological solutions at 37ºC. Our previous studies (Elkin et al., 2007; Elkin et al., 2010) reported modulus for slow (0.5-1Hz) indentations, which were considered to yield approximately static properties.

Using a similar approach which has been applied to single cells (Mahaffy et al., 2000; Mahaffy et al., 2004), we presented a methodology to measure viscoelastic properties of brain tissue. In the current study, we have extended our earlier results to dynamic indentations. These preliminary studies indicate that it will be possible to apply this technique to brain tissue to determine frequency dependent storage and loss moduli for subregions of the hippocampus using the AFM. We have shown previously that different regions within the adult hippocampus have significantly different mechanical properties. The CA1 region was much stiffer than the CA3 or DG regions, suggesting that the CA3 region and DG will deform to a greater extent than the CA1 *in vivo*.

One of the challenges with most indentation-based testing is identification of when the indenter contacts the specimen. One strategy is to identify a pre-load to indicate contact. This is analogous to determining a minimum static deflection of the AFM cantilever probe. The dynamic indentation tests also provide a second source of information that may be more sensitive that static deflection. As the probe is oscillated in fluid above the specimen before contact, the probe deflection is due to viscous drag in the fluid only. Hence its phase should be 90° compared to the driving oscillation. Upon contact with the specimen and excitation of the tissue, the deflection is now caused, in part, by its elastic deformation. The magnitude of the in-phase deflection should increases whereas the magnitude of the out-of-phase component should decrease. We continue to work on a robust and automated method for contact point identification.

We continue to generate the dynamic data for many regions of the brain. These properties can be incorporated into FE models which include detailed anatomical structures like the hippocampus. The FE output can then be more precisely compared to patterns of histological damage to determine its biofidelity.

CONCLUSION

We have used the AFM to measure mechanical properties of the brain within subregions overcoming challenges of spatial and force resolution. We hypothesize that the local mechanical properties could explain regional patterns of cell death after TBI. The AFM methodology was successfully extended to the viscoelastic regime up to a frequency of 800 Hz. In the future, these methods will be used to determine region-specific, storage and loss moduli for incorporation into FE models. These methods are applicable to tissue from other species and other ages so as to inform pediatric-specific models, as well.

ACKNOWLEDGEMENTS

This work was supported by the National Highway Traffic Safety Administration.

REFERENCES

Alcaraz J, Buscemi L, Grabulosa M, Trepat X, Fabry B, Farre R, Navajas D (2003) Microrheology of human lung epithelial cells measured by atomic force microscopy. Biophysical Journal 84:2071-2079.

Arbogast KB, Margulies SS (1997) Regional differences in mechanical properties of the porcine central nervous system. Stapp Car Crash Journal 41 293-300.

Brands DW, Bovendeerd PH, Peters GW, Wismans JS (2000) The large shear strain dynamic behavior of in-vitro porcine brain tissue and a silicone gel model material. Stapp Car Crash Journal 44 249-260.

Cater HL, Sundstrom LE, Morrison III B (2006) Temporal development of hippocampal cell death is dependent on tissue strain but not strain rate. Journal of Biomechanics 39:2810-2818.

Coats B, Margulies SS (2005) Material properties of porcine parietal cortex. J Biomech.

Costa KD (2003) Single-cell elastography: probing for disease with the atomic force microscope. DisMarkers 19:139-154.

Costa KD, Yin FC (1999) Analysis of indentation: implications for measuring mechanical properties with atomic force microscopy. Journal of Biomechanical Engineering 121:462-471.

Darvish KK, Crandall JR (2001) Nonlinear viscoelastic effects in oscillatory shear deformation of brain tissue. Medical Engineering and Physics 23:633-645.

Elkin BS, Ilankovan A, Morrison III B (2010) Age-dependent regional mechanical properties of the rat hippocampus and cortex. Journal of Biomechanical Engineering 132.

Elkin BS, Azeloglu EU, Costa KD, Morrison III B (2007) Mechanical heterogeneity of the rat hippocampus measured by AFM indentation. Journal of Neurotrauma 24:812-822.

Gefen A, Gefen N, Zhu Q, Raghupathi R, Margulies SS (2003) Age-dependent changes in material properties of the brain and braincase of the rat. Journal of Neurotrauma 20:1163-1177.

Hicks R, Soares H, Smith D, McIntosh T (1996) Temporal and spatial characterization of neuronal injury following lateral fluid-percussion brain injury in the rat. Acta Neuropathologica 91:236-246.

Hrapko M, van Dommelen JA, Peters GW, Wismans JS (2006) The mechanical behaviour of brain tissue: large strain response and constitutive modelling. Biorheology 43:623-636.

Lippert SA, Rang EM, Grimm MJ (2004) The high frequency properties of brain tissue. Biorheology 41:681-691.

Mahaffy RE, Shih CK, MacKintosh FC, Kas J (2000) Scanning probe-based frequency-dependent microrheology of polymer gels and biological cells. PhysRevLett 85:880-883.

Mahaffy RE, Park S, Gerde E, Kas J, Shih CK (2004) Quantitative analysis of the viscoelastic properties of thin regions of fibroblasts using atomic force microscopy. Biophysical Journal 86:1777-1793.

Morales DM, Marklund N, LeBold D, Thompson HJ, Pitkanen A, Maxwell WL, Longhi L, Laurer H, Maegele M, Neugebauer E, Graham DI, Stocchetti N, McIntosh TK (2005) Experimental models of traumatic brain injury: do we really need to build a better mousetrap? Neuroscience 136:971-989.

Morrison III B, Cater HL, Wang CB, Thomas FC, Hung CT, Ateshian GA, Sundstrom LE (2003) A tissue level tolerance criteria for living brain developed with an in vitro model of traumatic mechanical loading. Stapp Car Crash Journal 47:93-105.

Nicolle S, Lounis M, Willinger R (2004) Shear properties of brain tissue over a frequency range relevant for automotive impact situations: new experimental results. Stapp Car Crash Journal 48 239-258.

Nicolle S, Lounis M, Willinger R, Palierne JF (2005) Shear linear behavior of brain tissue over a large frequency range. Biorheology 42:209-223.

Prange MT, Margulies SS (2002) Regional, directional, and age-dependent properties of the brain undergoing large deformation. Journal of Biomechanical Engineering 124:244-252.

Smith DH, Chen XH, Xu BN, McIntosh TK, Gennarelli TA, Meaney DF (1997) Characterization of diffuse axonal pathology and selective hippocampal damage following inertial brain trauma in the pig. Journal of Neuropathology and Experimental Neurology 56:822-834.

Takhounts EG, Eppinger RH, Campbell JQ, Tannous RE, Power ED, Shook LS (2003) On the development of the SIMon finite element head model. Stapp Car Crash Journal 47 107-133.

Takhounts EG, Ridella SA, Hasija V, Tannous RE, Campbell JQ, Malone D, Danelson K, Stitzel J, Rowson S, Duma S (2008) Investigation of traumatic brain injuries using the next generation of simulated injury monitor (SIMon) finite element head model. Stapp Car Crash Journal 52:1-31.

Zhou C, Khalil TB, King AI (1995) A new model comparing impact responses of the homogenous and inhomogenous human brain. Stapp Car Crash Journal 39 121-129.